# Modeling Geologic Faulting in a Fractured Reservoir Simulator

Gavin Glenn and Neal Sams
United States Department of Energy
National Energy Technology Laboratory. Morgantown, WV
July 31, 2015

## I Abstract

NF FLOW is software created at the National Energy Technology Laboratory (NETL) that simulates fluid flow through naturally fractured reservoirs [3]. It relies on methods from computational fluid dynamics, such as the discretization of conservation equations and has been validated against historical reservoir data with good accuracy. This paper describes the addition of a simple geologic fault model into NF FLOW. The model was validated for small data sets and is presently being finalized for the next release of NF FLOW. The purpose of this study was to explore the feasibility of even a simple fault model in a fractured reservoir simulator, and its positive results open avenues for further research into a relatively unexplored area.

## II Introduction

Hydraulic fracturing is a process used to obtain underground fluid resources, such as natural gas or oil. By drilling vertical and horizontal wells into the Earth's surface, one is able to access a vast network of fractured rock layers. The wells and fractures together create flow paths for a desired resource [1]. Upon reaching the surface the fluid may be collected and processed. During its ascension, however, the resource may encounter many factors that influence its flow rate. While many of these factors have been previously considered in fluid flow models [2, 7] (NF FLOW included), this study focused on the less analyzed effects of geologic faulting in a reservoir. A geologic fault is a plane intersecting a volume of rock which may cause discontinuities between each side. When faulting occurs, the fracture network can change substantially, especially if layers shift along the fault with respect to one another [4].

## Fluid Flow Simulations

The general goal of most fluid simulations is to predict the rate at which fluid flows through a medium at a particular time [5, 6]. This rate is referred to as the production or performance of a reservoir. Calculation of production involves considering a number of physical factors such as the porosity and permeability of rock layers or the pressure field at a certain time. This study was particularly focused on a fault's effect on production, which was analyzed by integrating a new model into NF FLOW.

NF FLOW simulates fluid flow through a fractured reservoir by first reading in fracture data, rock layer information, and well descriptions. The fractures are represented as vertical planes with a very small thickness, and a single fracture may span multiple rock layers. The fractures are stochastically generated using the NETL software FRACGEN. This data is history matched based on parameters such as fracture density, length, and aperture. The goal of this process is to modify these parameters so that the model can predict reservoir performance for years to come. The descriptions of rock layers and wells may be taken from geologic records. Finally, the fault is defined by endpoints, a shift value, a hydraulic aperture, and a sealing factor. The fault's representation is consequentially very similar to a large fracture, but its intrinsic properties merit new geometric and physical considerations.

## Visualization

Depicted in Figure 1 is a 3D model of naturally fractured rock layers and a well shifted along a fault. The fault is modeled as a vertical plane spanning the entire fracture network. Thus, each side of the fault is able to be shifted along a line in the form $y = mx + b$.

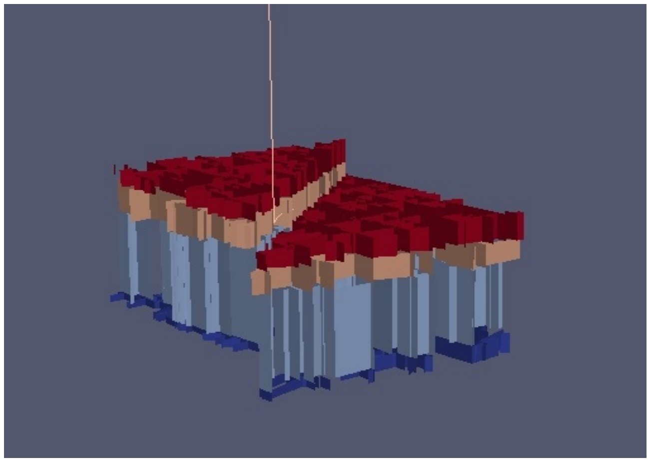

Figure 1: Rock layers (colored) shifted along a fault created in *Paraview*

The data used to create this visual model is an example of possible input for NF FLOW. As seen in the image, each side of the fault has lost and gained connections with the other. In particular, fractures from once disjointed layers may now intersect, or conversely, previously connected layers may no longer have any intersecting fractures. To complicate things further, properties of the fault can allow fluid to flow vertically and horizontally through the plane, so layers with no directly intersecting fractures may still have the ability to communicate.

As a consequence flow modeling through the fault is more involved, with each fracture that intersects the plane serving as a fluid source or sink. Understanding this change in communicability between layers, both due to a geometric shift as well as the fault's flow properties, is the crux of the problem. See Figure 2 for a closer look at how fractures hit and shift along the fault plane.

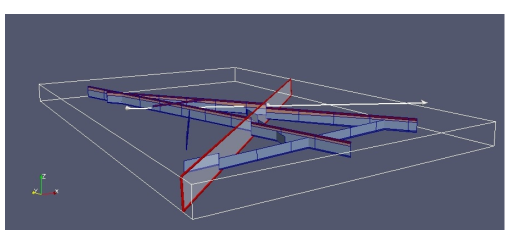

Figure 2: Fractures hitting a translucent fault plane created in *Paraview*

# III Fault Geometry

Our approach to the problem involves first developing an algorithm to handle the faulted geometry of the reservoir. In our simulation, fluid can travel through nodes–or locations where fractures intersect. When a fault is added, new nodes are formed along the fault. The general procedure is shown in figures 3 and 4 below.

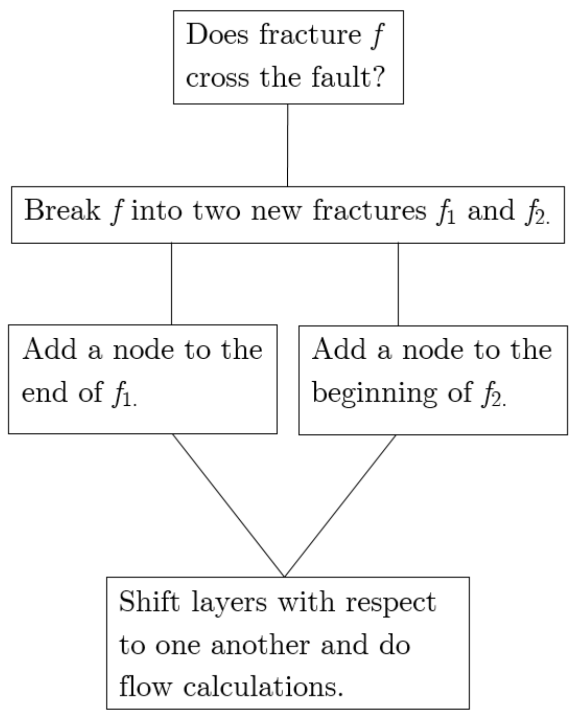


Figure 3: Fault Procedure

As seen in the images, fractures are broken to begin and end on each side of the fault. Next, a new network of nodes is formed where the fractures

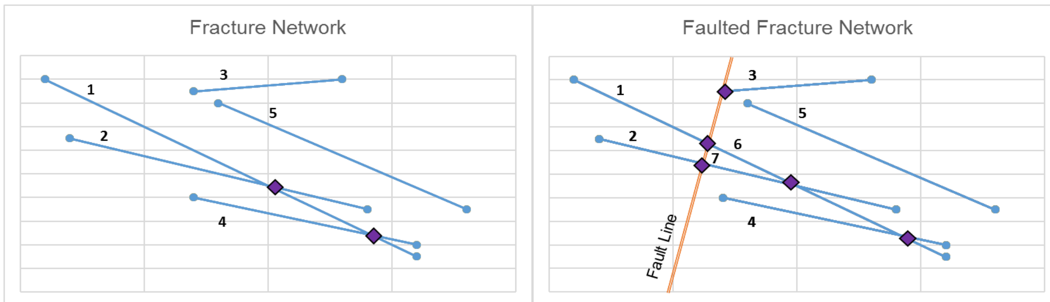


Figure 4: Map view of a fracture network before and after faulting. The diamonds represent nodes, and the numbers represent the fracture number.

intersect the fault. Finally, the vertical shift affects the interplay between the new nodes and fractures. After returning this information about the new nodes to the main program, we are now ready to proceed with flow calculations.

# IV Flow Continuity

By conservation of mass, the amount of fluid entering the fault plane from intersecting fractures must be equal to the amount leaving it. Thus, we employ the continuity equation to model flow through the fault. Recall the continuity equation for fluid dynamics:

$$\frac{\partial \rho}{\partial t} + \nabla \cdot (\rho \vec{v}) = 0$$

where $\rho$ is fluid density, $\vec{v}$ is the fluid velocity, and $t$ is time.

Though the fault is represented as a vertical plane, it is given a small hydraulic aperture for computations (since real world faults have some thickness). Nonetheless, flow through this minuscule distance is negligible compared to flow through the vertical and horizontal directions of the plane. For this reason we consider the continuity equation only in two dimensions, and from it we derive a finite difference equation for our computational simulation.

To discretize the problem, we first partition the fault plane into an $l$ x $m$ grid (see Figure 5 for an example) and placed node(s) at each block where fractures intersect. To simplify calculations we use a general index $k$ to represent a block's row and column position rather than the usual $(i, j)$ notation. The simple transformation being

$$k = m(i-1) + j$$

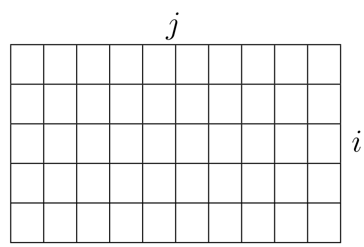


Figure 5: An example of a 5x10 figure

We begin our finite difference derivation with

$$\frac{\partial \rho}{\partial t} + \frac{\partial \rho v_x}{\partial x} + \frac{\partial \rho v_y}{\partial y} = \Sigma \tag{1}$$

where $\Sigma$ represents a sum of sink/source terms in the $x$ and $y$ directions. From the real gas equation,

$$\rho = \left(\frac{1}{RT}\right)\left(\frac{p}{Z}\right) \tag{2}$$

where $Z$ is the compressibility factor, $p$ is pressure, $R$ is the ideal gas constant, and temperature $T$ is constant for an isothermal reservoir. Substituting equation (2) into equation (1) and multiplying by $RT$ yields

$$\frac{\partial}{\partial t}\left(\frac{p}{Z}\right) + \frac{\partial}{\partial x}\left(\frac{p}{Z} v_x\right) + \frac{\partial}{\partial y}\left(\frac{p}{Z} v_y\right) = RT\Sigma \tag{3}$$

Fluid velocity through a porous medium is given by Darcy's Law*, which states

$$\vec{v} = -\frac{\kappa}{\mu}\nabla p \tag{4}$$

where $\kappa$ is the intrinsic permeability of the medium and $\mu$ is viscosity. Making this substitution for velocity into equation (3) gives us

$$\frac{\partial}{\partial t}\left(\frac{p}{Z}\right) - \frac{\partial}{\partial x}\left(\frac{\kappa p}{\mu Z}\frac{\partial p}{\partial x}\right) - \frac{\partial}{\partial y}\left(\frac{\kappa p}{\mu Z}\frac{\partial p}{\partial y}\right) = RT\Sigma \tag{5}$$

To linearize our spatial terms, we define the potential $\Phi$ with the following Kirchhoff transformation on $p$

$$\Phi(p) := \int_0^p \frac{p' dp'}{\mu(p')Z(p')} \tag{6}$$

By the chain rule and the fundamental theorem of calculus,

$$\frac{\partial \Phi}{\partial x} = \frac{\mathrm{d}\Phi}{\mathrm{d}p}\cdot\frac{\partial p}{\partial x} = \left(\frac{\mathrm{d}}{\mathrm{d}p}\int_0^p \frac{p' dp'}{\mu(p')Z(p')}\right)\cdot\frac{\partial p}{\partial x} = \left(\frac{p}{\mu Z}\right)\frac{\partial p}{\partial x} \tag{7}$$

The partial of $\Phi$ with respect to $y$ is similar, so we substitute into equation (5) to obtain

$$\frac{\partial}{\partial t}\left(\frac{p}{Z}\right) - \frac{\partial}{\partial x}\left(\kappa\frac{\partial \Phi}{\partial x}\right) - \frac{\partial}{\partial y}\left(\kappa\frac{\partial \Phi}{\partial y}\right) = RT\Sigma \tag{8}$$

We let $z$ be the fault aperture and integrate both sides over a volume $V = z\Delta x\Delta y$

$$\int \frac{\partial}{\partial t}\left(\frac{p}{Z}\right)dV - \int \frac{\partial}{\partial x}\left(\kappa\frac{\partial \Phi}{\partial x}\right)dV - \int \frac{\partial}{\partial y}\left(\kappa\frac{\partial \Phi}{\partial y}\right)dV = RT\int \Sigma dV$$

*Darcy's Law actually reads $\vec{v} = -\phi\frac{\kappa}{\mu}\nabla p$.
In our case fault porosity $\phi = 1$

$$= V\frac{\partial}{\partial t}\left\langle \frac{p}{Z} \right\rangle_{i,j} - \kappa z \Delta y \left[ \left.\frac{\partial \Phi}{\partial x}\right|_{x^+} - \left.\frac{\partial \Phi}{\partial x}\right|_{x^-} \right] - \kappa z \Delta x \left[ \left.\frac{\partial \Phi}{\partial y}\right|_{y^+} - \left.\frac{\partial \Phi}{\partial y}\right|_{y^-} \right] = S_{i,j} \tag{9}$$

where $S_{i,j}$ represents an average of sink and source terms of $\vec{v}$ and $\vec{\rho}$ over the fault aperture $z$ and $\left\langle \frac{p}{Z} \right\rangle_{i,j}$ is the average value of $\frac{p}{Z}_{i,j}$. Using our index transformation, equation (9) becomes

$$V\frac{\partial}{\partial t}\left\langle \frac{p}{Z} \right\rangle_{k} - \kappa z \Delta y \left[ \left.\frac{\partial \Phi}{\partial x}\right|_{x^+} - \left.\frac{\partial \Phi}{\partial x}\right|_{x^-} \right] - \kappa z \Delta x \left[ \left.\frac{\partial \Phi}{\partial y}\right|_{y^+} - \left.\frac{\partial \Phi}{\partial y}\right|_{y^-} \right] = S_k \tag{10}$$

We want to consider $\Phi$ at each fault grid block and $\frac{p}{Z}$ at time steps $t$ and $t+1$. The general case representing the potential at the $k$th block is depicted below.

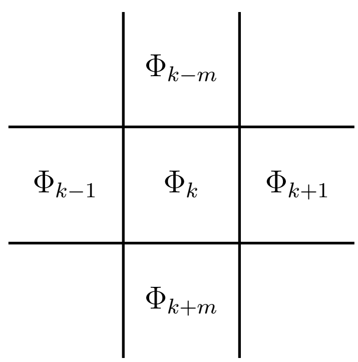


That is, if fluid potential passes through block $k$, it also passes through up to 4 other contiguous blocks. For the blocks around the border of the fault grid, appropriate $\Phi$ terms become zero. Using these considerations we discretize equation (10) and obtain

$$\frac{V}{\Delta t}\left[\left(\frac{p}{Z}\right)_k^{t+1} - \left(\frac{p}{Z}\right)_k^{t}\right] - \frac{\kappa z \Delta y}{\Delta x}\left[\left(\Phi_{k+1}^{t+1} - \Phi_k^{t+1}\right) - \left(\Phi_k^{t+1} - \Phi_{k-1}^{t+1}\right)\right]$$
$$- \frac{\kappa z \Delta x}{\Delta y}\left[\left(\Phi_{k+m}^{t+1} - \Phi_k^{t+1}\right) - \left(\Phi_k^{t+1} - \Phi_{k-m}^{t+1}\right)\right] - S_k = 0 \tag{11}$$

Letting $T_x = \frac{\kappa z \Delta y}{\Delta x}$, $T_y = \frac{\kappa z \Delta x}{\Delta y}$, and $\mathbf{\Phi}$ be the vector with components $\Phi_k$ we arrive at our final discretized continuity equation.

$$f_k(\mathbf{\Phi}) = \frac{V}{\Delta t}\left[\left(\frac{p}{Z}\right)_k^{t+1} - \left(\frac{p}{Z}\right)_k^{t}\right] + T_x(\Phi_k^{t+1} - \Phi_{k+1}^{t+1}) + T_x(\Phi_k^{t+1} - \Phi_{k-1}^{t+1})$$
$$+ T_y(\Phi_k^{t+1} - \Phi_{k+m}^{t+1}) + T_y(\Phi_k^{t+1} - \Phi_{k-m}^{t+1}) - S_k = 0 \tag{12}$$

We are interested in finding the value of $\mathbf{\Phi}$ such that

$$f_k(\mathbf{\Phi}) = 0 \tag{13}$$

for all values of $k$. This is simply a system of nonlinear equations, so we employ Newton's method. We pick an initial guess $\mathbf{\Phi}_0$ (that is, $\mathbf{\Phi}$ at time step $t = 0$) based on initial conditions from the reservoir and ultimately find an iterative solution to the vector equation

$$J\left[f(\mathbf{\Phi}_t)\right]\Delta\mathbf{\Phi} = -f(\mathbf{\Phi}_t) \tag{14}$$

where $\Delta\mathbf{\Phi} = \mathbf{\Phi}_{t+1} - \mathbf{\Phi}_t$ and $J$ is the Jacobian matrix of $f$ given by

$$J\left[f(\mathbf{\Phi}_t)\right] = \begin{pmatrix} \frac{\partial f_1}{\partial \Phi_1}(\mathbf{\Phi}_t) & \frac{\partial f_1}{\partial \Phi_2}(\mathbf{\Phi}_t) & \dots & \frac{\partial f_1}{\partial \Phi_n}(\mathbf{\Phi}_t) \\ \frac{\partial f_2}{\partial \Phi_1}(\mathbf{\Phi}_t) & \frac{\partial f_2}{\partial \Phi_2}(\mathbf{\Phi}_t) & \dots & \frac{\partial f_2}{\partial \Phi_n}(\mathbf{\Phi}_t) \\ \vdots & \vdots & \ddots & \vdots \\ \frac{\partial f_n}{\partial \Phi_1}(\mathbf{\Phi}_t) & \frac{\partial f_n}{\partial \Phi_2}(\mathbf{\Phi}_t) & \dots & \frac{\partial f_n}{\partial \Phi_n}(\mathbf{\Phi}_t) \end{pmatrix} \tag{15}$$

Once a solution for $\mathbf{\Phi}$ is obtained, we can numerically invert our transform to calculate the pressure field for the fault at a desired time step. Finally, we pass this information back to the main program.

# V Results and Conclusions

In order to validate our model on an qualitative level, we performed a series of "reasonableness tests" with a small data set. For example, a sealing fault–which allows little fluid to pass through–should decrease a reservoir's performance. This sealing parameter $r$ is usually determined from geologic field data. It appears in the equation

$$\kappa = r\left(\frac{z^2}{12}\right) \tag{16}$$

and is used to calculate the parameter $\kappa$ seen earlier in our derivation. $r$ takes values between 0 and 1. The closer $r$ is to 1, the more sealed the fault is. Figure 6 shows the model's output for low and high sealing factors, respectively.

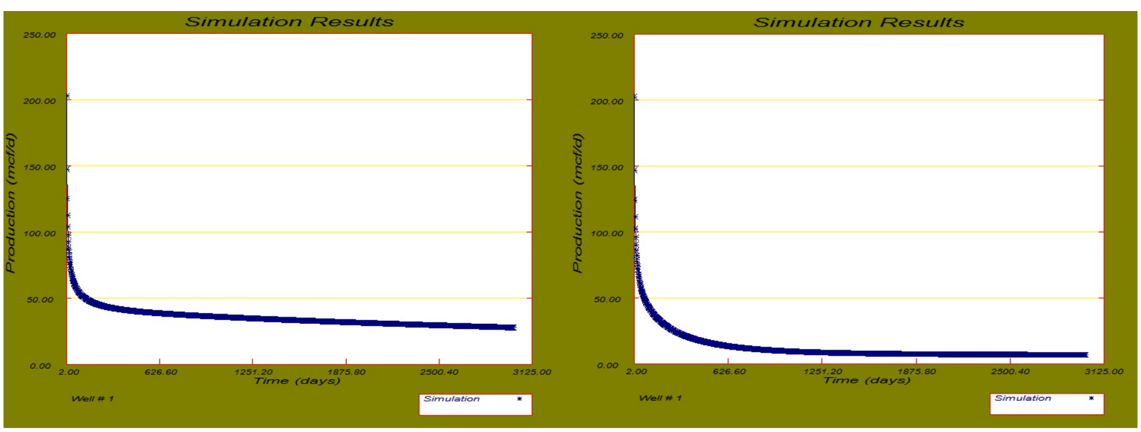


Figure 6: The left image is the model's output for a low sealing factor; the right is output for a high sealing factor

As seen in the images, the sealing fault decreased the reservoir's production substantially, as expected. In addition, the fact that the sealing fault was not completely sealed ($r$ close to but not equal to 1) is responsible for the graph's long "tail." These and other reasonableness tests were used to verify our model conceptually. The main product of our study is the discovery that adding a valid fault model to a reservoir simulator is possible. While our model makes some assumptions, it nonetheless illuminates the potential for further fault modeling and research–a subject which has remained largely unstudied. Future research could include improving upon our main simplification: the fault's representation. We idealized the fault's orientation as a vertical plane and its aperture as a uniform distance between two parallel plates. In reality, many faults have an angle and some roughness along their boundaries. Further, our results are presently very qualitative. As the model's code is finalized, we plan on obtaining more quantitative results with real data sets. The interested reader should see reference [3] to download and use NF FLOW.

# VI References


[1] Rachel Curtis. What is horizontal drilling, and how does it differ from vertical drilling? Institute for Energy and Environmental Research of Northeastern Pennsylvania Clearinghouse. http:energy.wilkes.edu/158.asp. 2011.

[2] Jihoon Kim and George J. Moridis. Numerical analysis of fracture propagation during hydraulic fracturing operations in shale gas systems. *International Journal of Rock Mechanics and Mining Sciences*, 76:127 – 137, 2015.

[3] U.S. Department of Energy. Discrete fracture reservoir simulator. http://www.netl.doe.gov/research/on-site-research/research-portfolio/discrete-fracture-reservoir-simulation.

[4] U.S. Department of the Interior. Fault-geologic glossary. http://geomaps.wr.usgs.gov/parks/deform/gfaults.html. 2014.

[5] Varahanaresh Sesetty and Ahmad Ghassemi. A numerical study of sequential and simultaneous hydraulic fracturing in single and multi-lateral

horizontal wells. *Journal of Petroleum Science and Engineering*, 132:65 – 76, 2015.

[6] Yu-Shu Wu and Karsten Pruess. A numerical method for simulating non-newtonian fluid flow and displacement in porous media. *Advances in Water Resources*, 21(5):351 – 362, 1998.

[7] Wu Yi, Liu Hong, Si Yong, and Pang Jin. Physical simulation for water injection of horizontal wells in naturally fractured buried- hill reservoirs. *Energy Procedia*, 16, Part B:1364 – 1371, 2012. 2012 International Conference on Future Energy, Environment, and Materials.